Deriving pulsar pair-production multiplicities from pulsar wind nebulae using H.E.S.S. and LHAASO observations

S. T. Spencer &

Erlangen Centre for Astroparticle Physics (ECAP)

A. M. W. Mitchell

Department of Physics, Clarendon Laboratory

Arxiv: 2502.01318

Reporter: 曹顺顺 (Shunshun Cao)

2025.2

12 pages in total

I. Introduction

Pulsar wind nebulae (脉冲星星风云，PWNe):
处在脉冲星周围的，由脉冲星星风作为能量来源的，发光的云状天体。

A note in Zhihu
for Amato’s paper.

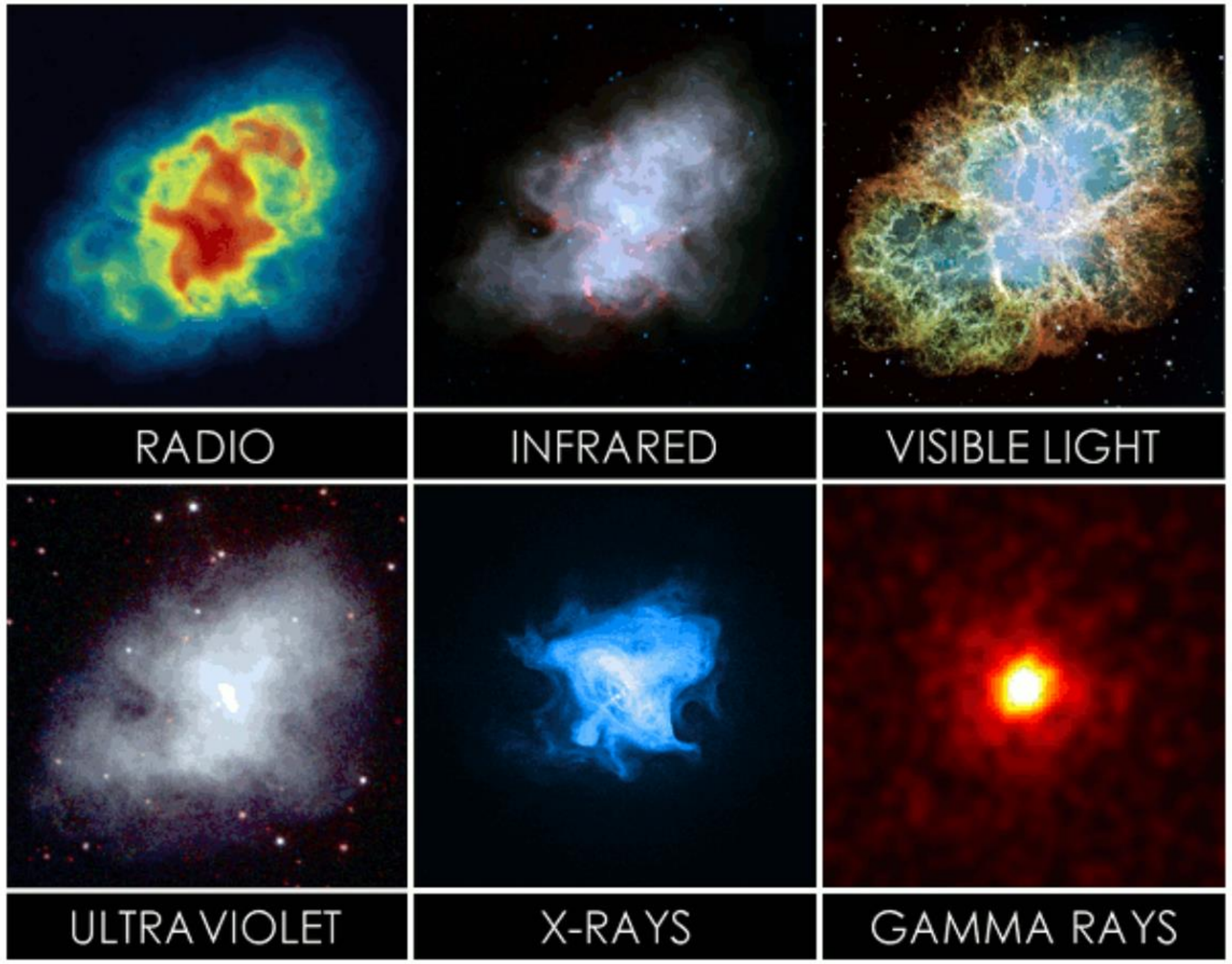

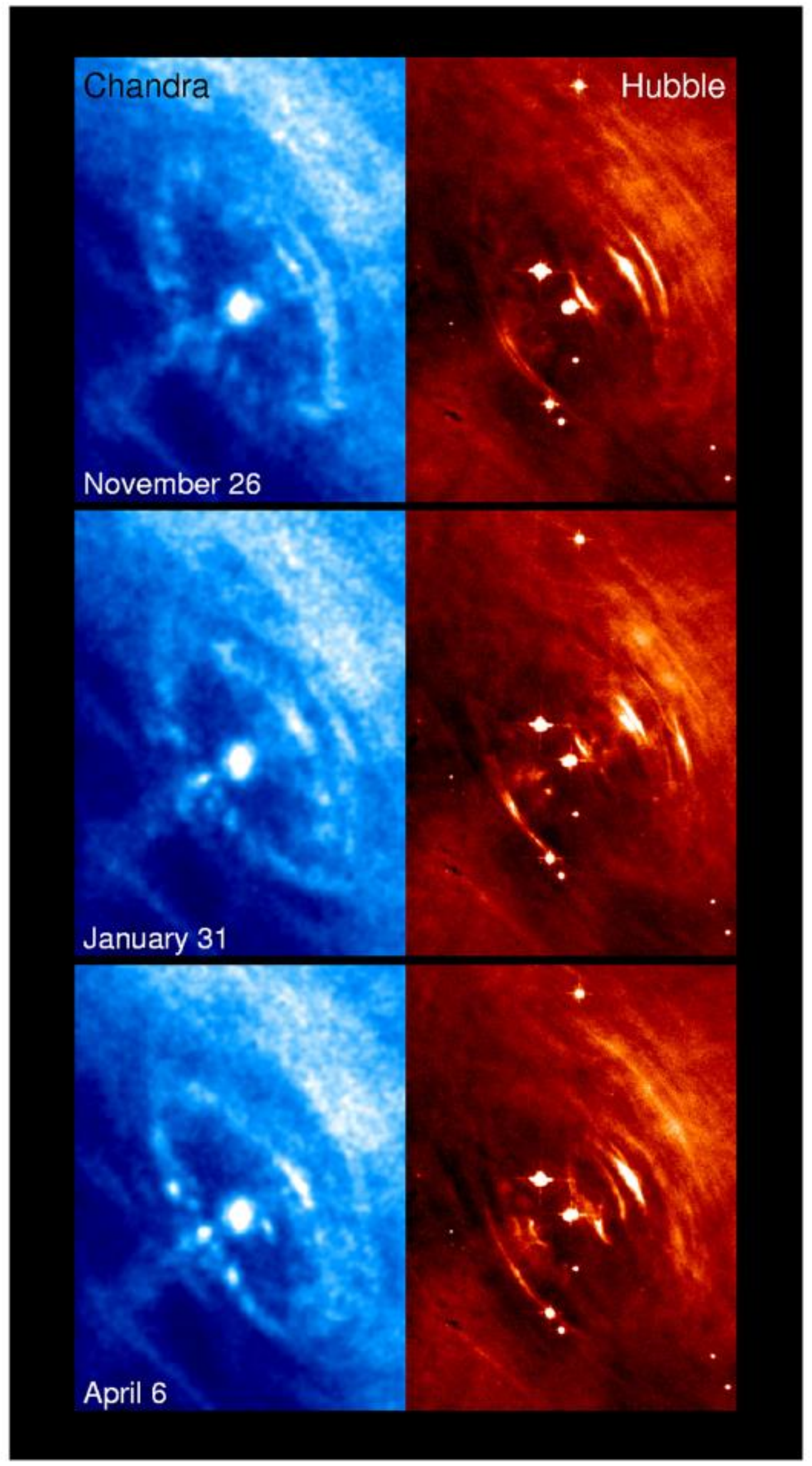

Amato 2024 arxiv.

· Located within or out of supernova remnants (SNRs).

· Broadband emission.

· Most numerous class of galactic VHE γ-ray emitters.

(VHE: 0.1 TeV – 100 TeV)

VHE emission mechanisms: mainly two approaches

· Leptonic process: inverse Compton scattering (ICS) by electrons/positrons.

· Hadronic process: pion decays, where pions are created in proton collisions.

Source of electrons: compact star itself & pair creation (γ-B process)
Source of protons: compact star itself?

➔ Will **hadrons** escape the pulsar surface into the PWN?

A related quantity: average pair production multiplicity
$< \kappa > =$ (Number of e± escaping light cylinder)
/(Number of Goldreich-Julian e±)

[Hadrons do not multiply in cascades in magnetospheres.]

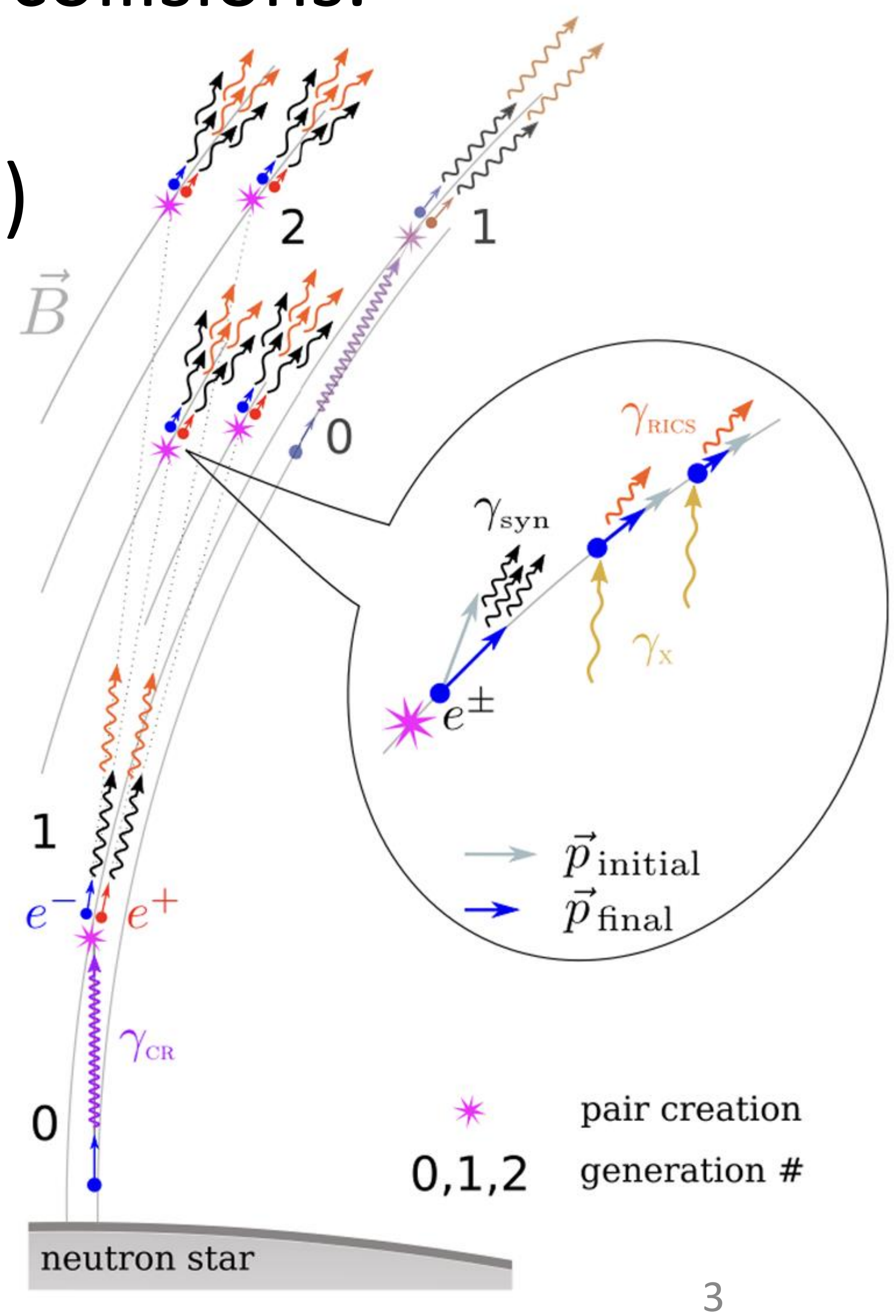

Goal of this paper: constrain <κ> for a number of PWNe.

Data from H.E.S.S. & LHAASO, also using radio observations (to get the sizes of PWNe & SNRs).

Modeling based on de Jager 2007 *ApJ*.

Basic logic:

$$\langle\kappa\rangle = \frac{N_{el}}{2N_{GJ}}$$

Number of PWN electrons: from observed spectrum
(Radiative spectrum ← electron spectrum → electron number)

Number of GJ electrons: from integrating E-dot
(Pulsar spin down ← Pulsar current → GJ electron number)

Note that this multiplicity is a lower limit, because PWN electrons are only calculated from VHE observations. They are only part of the total electrons.

II. Modeling theory

(i) Deriving P0:

Since the total GJ electron number needs accurate age information,
the initial/birth period P0 is required.

$$\frac{1}{2}I\left(\frac{2\pi}{P_0}\right)^2 - \frac{1}{2}I\left(\frac{2\pi}{P_t}\right)^2 = E_{SD}\ (E_*)$$ (total spin-down energy)

The E_{SD} is related to observables by pressure balance (all assuming spherical):

Central pressure of the SNR (Sedov solution): $P_{\rm snr} \simeq 0.074 E_0/R_{\rm snr}^3$

PWN interior pressure: $P_{\rm pwn} \simeq \frac{3(\gamma-1)}{4\pi}\frac{E_*}{R_{\rm pwn}^3}$

Equate two pressures: $R_{PWN}(t) = \eta_3(t)(\eta_1 E_{SD}/E_0)^{1/3} R_{SNR}(t).$ $\eta_1 = 1$ $\eta_3 = 1.02$

➔➔➔ $$P_0 = 2\pi\left[\frac{2E_0}{\eta_1 I}\left(\frac{R_{PWN}}{\eta_3 R_{SNR}}\right)^3 + \left(\frac{2\pi}{P_t}\right)^2\right]^{-1/2}$$

Also refer to van der Swaluw & Wu 2001 *ApJ*.

(ii) Deriving N_{GJ}

$\rho_{GJ} = -\dfrac{\vec{\Omega}\cdot\vec{B}}{2\pi c}$ Integrate ρ_{GJ}/e over the polar cap, times *c* ➔ $\dot{N}_{GJ} = \dfrac{B_\star \Omega^2 R_\star^3}{2\ e\ c}$

Plug in dipolar radiation loss: $\dot{E} = \dfrac{B_\star^2 R_\star^6 \Omega^4 \sin^2\chi}{6c^3}$ (sin^2 ~ ½)

Integrate over time➔➔➔ $N_{GJ} = \displaystyle\int_{t=0}^{t=-\tau(P_0)} \frac{[6c\dot{E}(t)]^{1/2}}{e}(-dt)$

E-dot changes because Ω changes with time (braking).

$\dot{\Omega} = -k\ \Omega^n$ ➔ $\Omega(t) = \dfrac{\Omega_0}{(1+t/\tau)^{1/(n-1)}}$ ➔ $\dot{E}(t) = \dot{E}_0\left(1+\dfrac{t}{\tau_0}\right)^{-\alpha}$

$\alpha = (n+1)/(n-1)$

$\tau_0 = P_0/((n-1)\dot{P}_0)$

In the present paper, $n = 3, \tau_0 = 10^3$yr.

Actual age used in integration: $\tau(P_t, \dot{P}_t, P_0, n) = \left(1 - \left(\dfrac{P_0}{P_t}\right)^{n-1}\right) \times \dfrac{P_t}{(n-1)\dot{P}_t}$

Also refer to Amato 2024 arxiv.

(ii) Deriving N_{el} and $\langle\kappa\rangle$

The observed radiation spectrum is related to the electron spectrum through one-zone model:

$$N(\epsilon, t) = \int_{t_i}^{t} dt_i Q[\epsilon_i(\epsilon, t; t_i), t_i] \frac{\partial \epsilon_i}{\partial \epsilon} \qquad \int d\epsilon_i \epsilon_i Q(\epsilon_i, t_i) = E_{Total} \qquad E_{\text{Total}} = \dot{E}\tau_c$$

$\partial\epsilon_{\mathrm{i}}/\partial\epsilon$ is determined by electron emission mechanisms (synchrotron, ICS) and system expanding.

e.g. (from Amato 2024 arxiv.) $$\frac{d\epsilon}{dt} = -\frac{\epsilon}{3R_N(t)}\frac{dR_N}{dt} - \frac{\sigma_T c}{8\pi(m_e c^2)^2}(\sqrt{2/3}B_N(t))^2\epsilon$$

Results on total PWN electron number :
(Giacinti et al. 2020, Woo et al. 2023, Amenomori et al. 2023, H.E.S.S. Collaboration et al. 2019)

$$N_{el} = E_{tot}\left(\frac{(2-\Gamma)E_0^{1-\Gamma}}{E_2^{2-\Gamma} - E_1^{2-\Gamma}}\right) \times \left(\frac{(E_2/E_0)^{1-\Gamma} - (E_1/E_0)^{1-\Gamma}}{1-\Gamma}\right)$$ Most H.E.S.S. sources

$$N_{el} \propto \left[\frac{1}{1-\Gamma}\left(\frac{E_2}{E_0}\right)^{1-\Gamma} - \frac{1}{1-\Gamma}\left(\frac{E_1}{E_0}\right)^{1-\Gamma}\right]$$ J1849-0001

$$N_{el} \propto \int_{E_0}^{E_2} \left(\frac{E}{E_1}\right)^{-\Gamma} \exp\left(\frac{E}{E_{cut}}\right) dE$$ J2021+3651

$$N_{el} \propto \left[\int_{E_0}^{E_1} E^{-\Gamma} dE + \int_{E_1}^{E_2} E^{-\Gamma_2} dE\right]$$ J1826-1334

III. Results

ATNF Name	R_{SNR} [pc]	R_{PWN} [pc]	P_t [ms]	$\dot{P}_t$ [$\times 10^{-13}$ s/s]	Model	E_0 [TeV]	E_1 [TeV]	E_{cut} [TeV]	E_2 [TeV]	Γ	Γ_2	Refs.
J1833-1034	2.98	0.8	61.8	2.02	BPL1	0.1	0.39	-	10	2.2	-	1, 2
J1513-5908	38.4	19.2	151.6	15.3	BPL1	0.1	0.61	-	10	2.2	-	1, 2
J1930+1852	10.8	2.7	136.9	7.50	BPL1	0.1	0.89	-	10	2.2	-	1, 2
J1846-0258	2.6	0.58	326.6	71.1	BPL1	0.1	0.40	-	10	2.2	-	1, 2
J0835-4510	19.5	12.2	89.3	1.25	BPL1	0.1	0.61	-	10	2.2	-	1, 2
J1747-2809	19.8	2.5	52.2	1.56	BPL1	0.1	0.17	-	10	2.2	-	1, 3
J2021+3651	-	-	103.7	0.957	PLEC	1	25	900	1400	1.4	-	4
J1841-0345	-	-	112.9	1.55	PLEC	1×10^{-5}	7.0	72	740	2.2	-	5
J1849-0001	-	-	38.5	0.142	PL	0.5	10	-	100	2.5	-	6
J1826-1334	-	-	101.5	0.753	BPL2	0.7	0.9	-	42	1.4	3.25	7

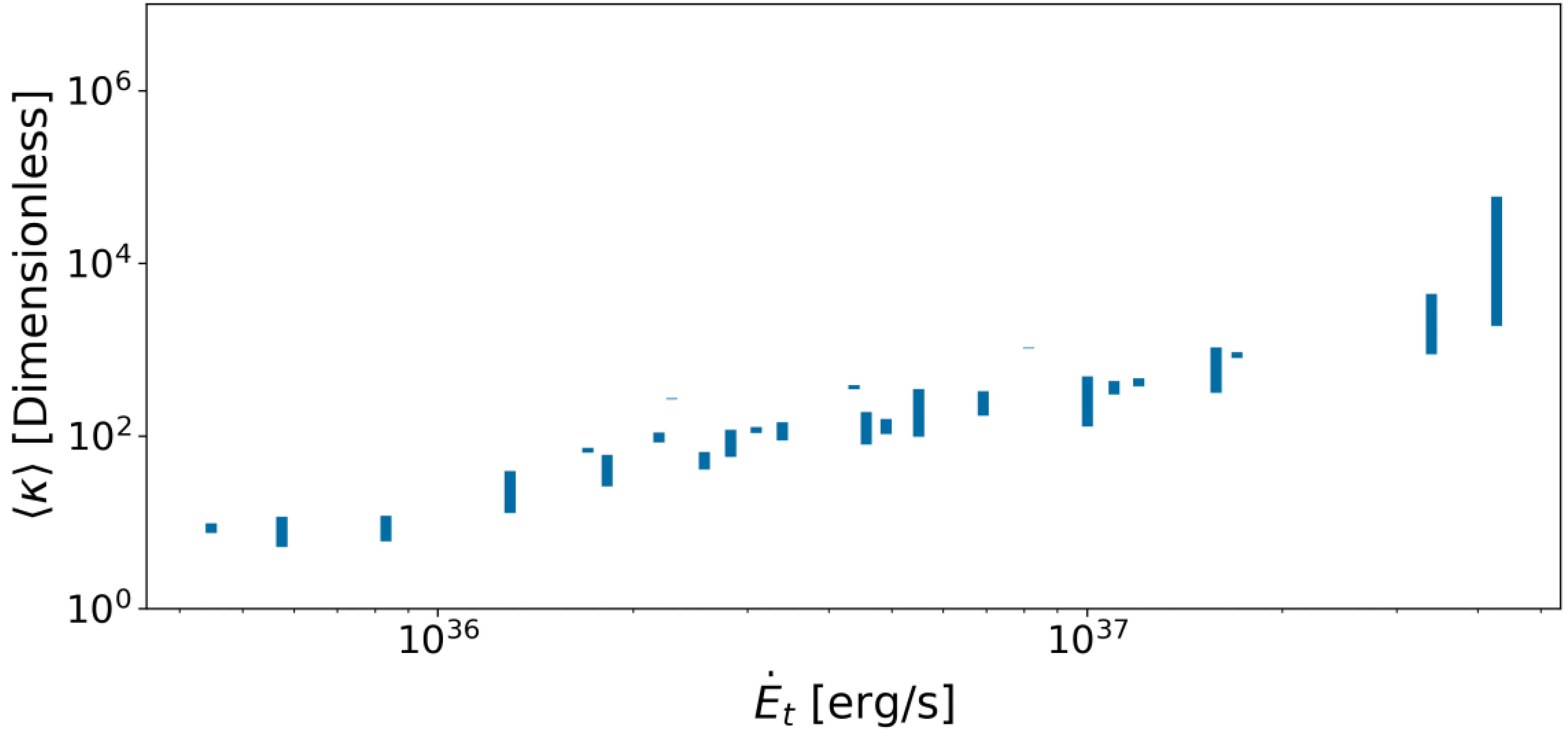

ATNF Name	P_0 [ms]	$\dot{E}_t$ [$\times 10^{36}$ erg/s]	N_{el} [$\times 10^{47}$ Counts]	$E_{\mathrm{e,tot}}$ [$\times 10^{47}$ erg]	$\langle\kappa\rangle$ [Dimensionless]
J1833-1034	33.0	33.9	45.6	51.8	1476
J1513-5908	15.2	17.0	5.14	8.35	809
J1930+1852	41.3	12.0	5.06	11.0	432
J1846-0258	50.8	8.13	1.62	1.87	1061
J0835-4510	10.9	6.92	18.7	1.87	174
J1747-2809	47.9	42.7	125	71.4	29328

The ↑ in the right two plots are derived from:

$$E_{\mathrm{CR}} \approx 1.2 \times 10^{20} A_{56} \eta \langle\kappa\rangle_{\mathrm{lim},4} I_{45} B_{13}^{-1} R_{\star,6}^{-3} \tau_{7.5}^{-1}$$

(Kotera, Amato & Blasi 2015 *JCAP*)

Iron cosmic ray could be **photodissociated** in the pulsar vicinity.

κ is related to radiation. The above equation describes the maximum <κ> to allow comic ray (iron) energy E_{CR} to escape.

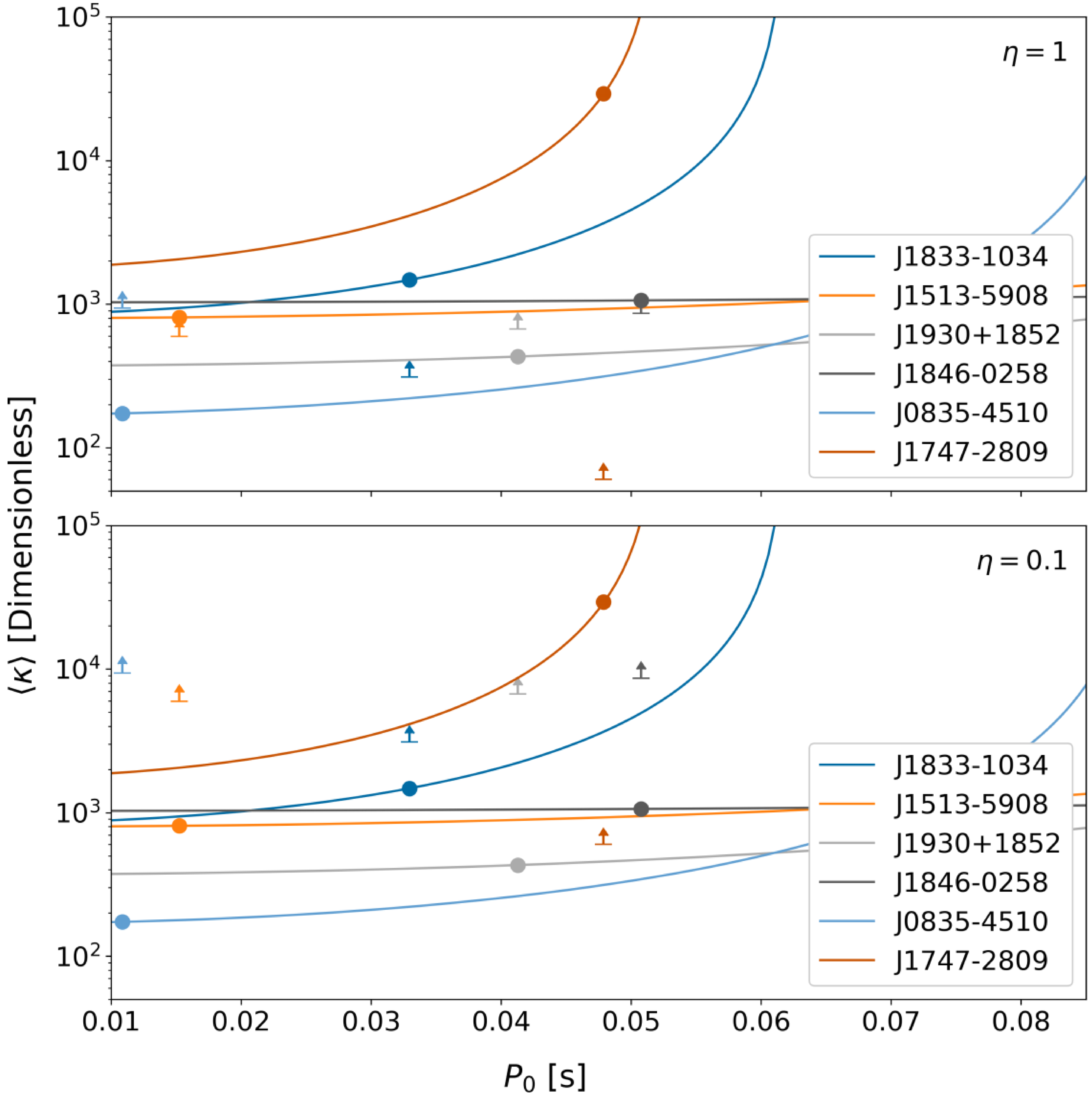

ATNF Name	P_0 [ms]	$\dot{E}_t$ [$\times 10^{36}$ erg/s]	N_{el} [$\times 10^{47}$ Counts]	$E_{\mathrm{e,tot}}$ [$\times 10^{47}$ erg]	$\langle\kappa\rangle$ [Dimensionless]
J1833-1034	33.0	33.9	45.6	51.8	1476
J1513-5908	15.2	17.0	5.14	8.35	809
J1930+1852	41.3	12.0	5.06	11.0	432
J1846-0258	50.8	8.13	1.62	1.87	1061
J0835-4510	10.9	6.92	18.7	1.87	174
J1747-2809	47.9	42.7	125	71.4	29328

Circular dots: <κ> derived through the method in Section II.

If <κ> is above <κ>lim, hadrons are less likely to escape into PWN.

For J1747-2809, it seems to be this case.

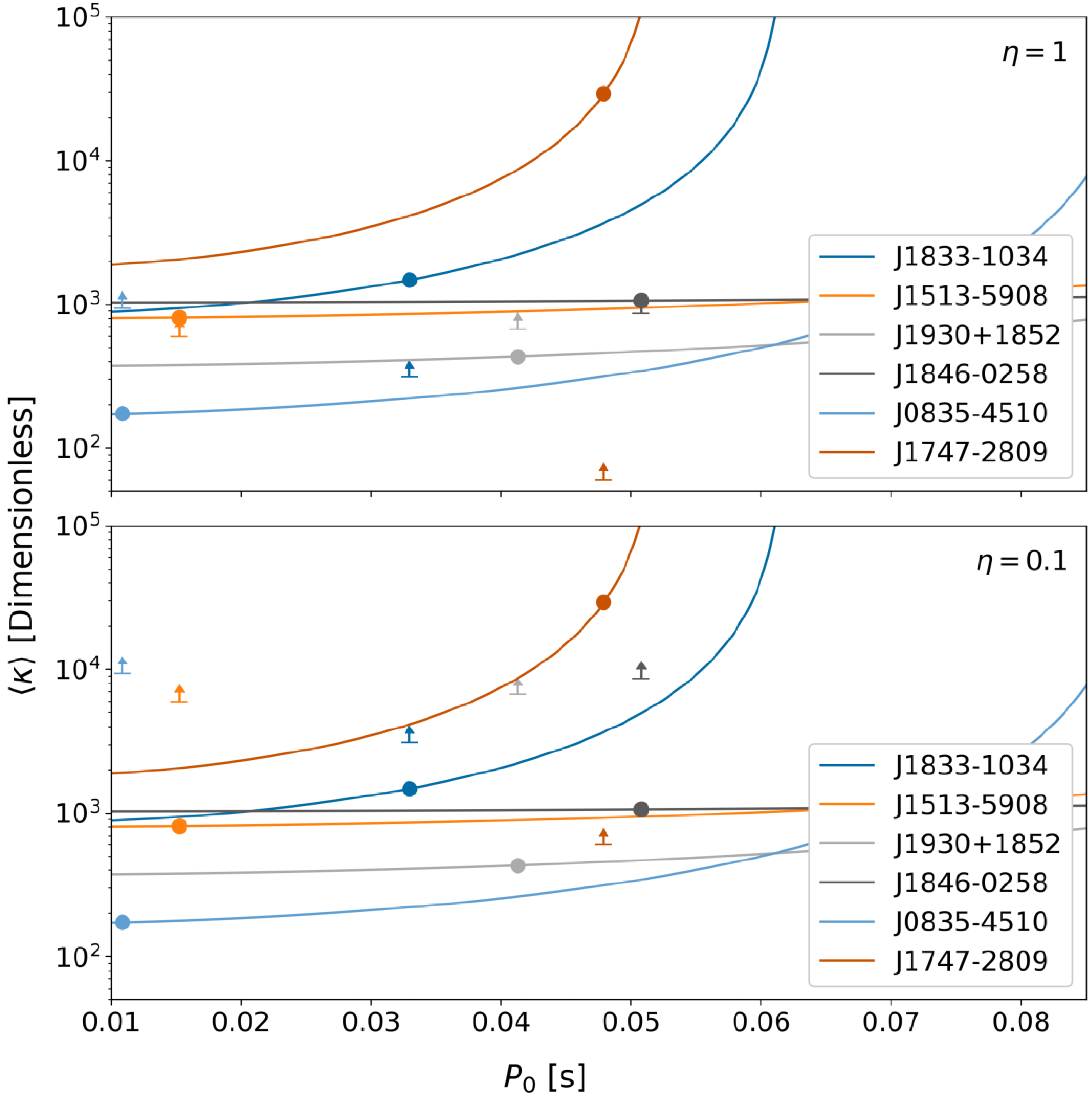

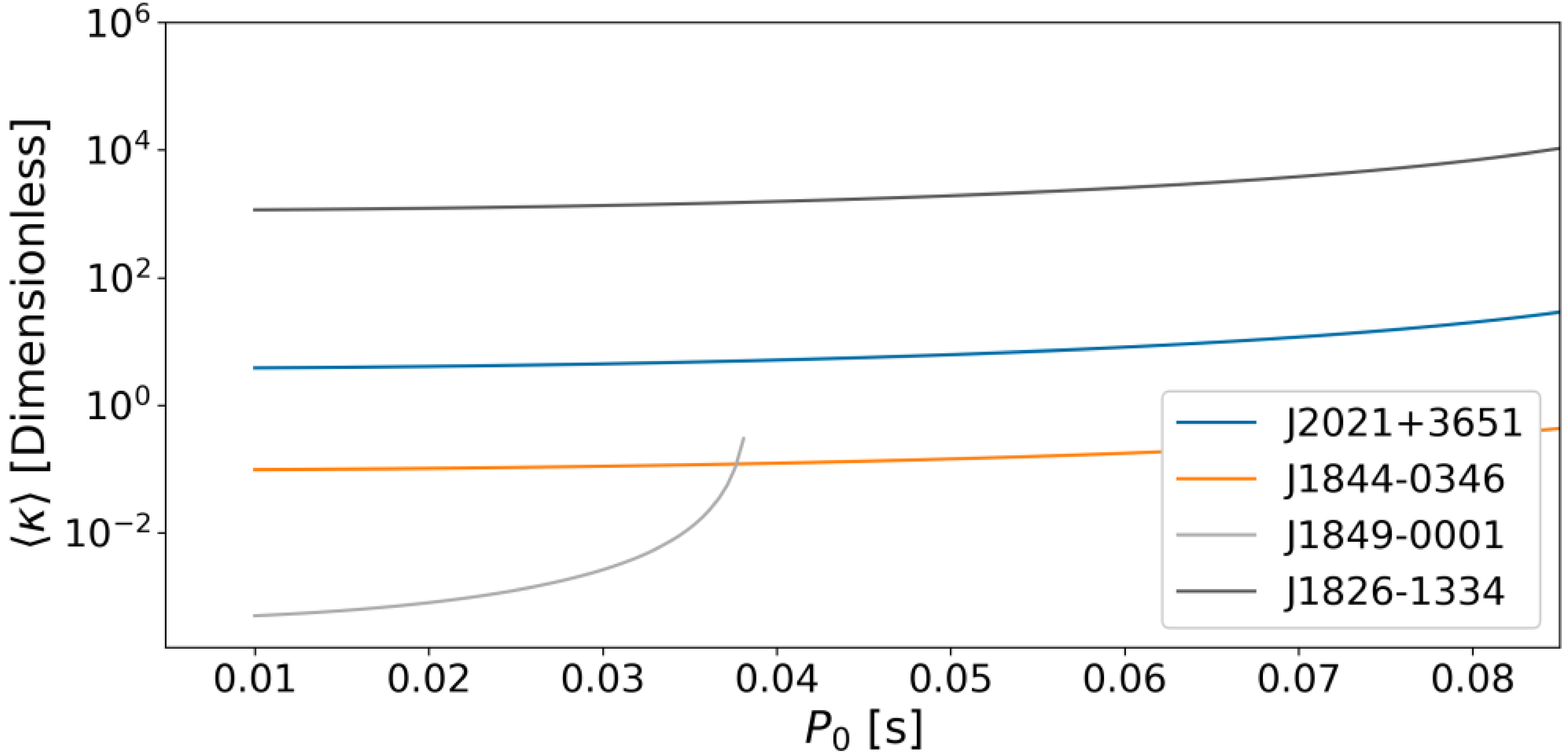

<κ> v.s. P_0 for four LHAASO sources.
Due to lack of radio observations, SNR & PWN sizes are unknown. No reliable P_0 is estimated.

➔ Radio interferometric images are required in the future.

In addition…

Parameter spaces